THE ASTROPHYSICAL JOURNAL, 425:43–50, 1994 April 10

THE FLATTENING DISTRIBUTION OF DWARF ELLIPTICAL GALAXIES IN THE VIRGO CLUSTER

BARBARA S. RYDEN[1,2] AND DONALD M. TERNDRUP[2,3]
Department of Astronomy, The Ohio State University, 174 West 18th Avenue, Columbus, OH 43210
Received 1993 August 6; accepted 1993 October 13

ABSTRACT

We have obtained *R*-band surface photometry of 70 dwarf elliptical galaxies in the Virgo Cluster. We find, in contrast to the results of earlier studies, that the dwarfs have a markedly flatter distribution of ellipticities than either "normal" elliptical galaxies or brightest cluster ellipticals. The ensemble of nucleated dwarfs is rounder than the non-nucleated galaxies. Neither the nucleated nor the nonnucleated dwarfs, however, have distributions as round as giant ellipticals

Subject headings: galaxies: clusters (Virgo) — galaxies: elliptical and lenticular, cD — galaxies: photometry — galaxies: structure

1. INTRODUCTION

The study of dwarf galaxies has a rich history, and despite many years of observational and theoretical effort there remains much to learn. One subject in particular—the origin of the dwarf systems—has received considerable attention throughout the years. Why are there, for example, both dwarf elliptical (dE) and dwarf irregular galaxies, and why do many dE's have unresolved nuclei in their cores? Do the different types of dwarf galaxies represent different ways of making galaxies, or different evolutionary stages of one type of galaxy? Are the dE's simply small versions of "normal" ellipticals (E's), or are they formed in a different fashion?

One of nature's best (or at least most convenient) laboratories for studying dwarf galaxies is the Virgo Cluster, and consequently many papers have been written about the Virgo dE's. Research in this area has been greatly aided by the publication of the extensive Virgo Cluster Catalog (VCC) by Binggeli, Sandage, & Tammann (1985, hereafter BST). Subsequent publications by these authors and collaborators have provided us with a wealth of new information.

Some of the more significant results concerning Virgo dE's can be briefly stated. The dE's are distinguished from E's by their low surface brightness (Reaves 1956, 1983; BST). Their brightness profiles are typically exponential, though many can be better described by $r^{1/4}$ profiles (Caldwell 1983; Binggeli, Sandage, & Tarenghi 1984; Ichikawa, Wakamatsu, & Okamura 1986; Impey, Bothun, & Malin 1988; Binggeli & Cameron 1991; James 1991). About 65% of the dE's with total blue magnitude $B_T \leq 18$ are nucleated, with the nucleation fraction nearly 100% for the brightest dE's and falling to 20% at $B_T = 18$ (BST, van den Bergh 1986). Nucleated dE's and faint ($B_T > 17.5$) nonnucleated dE's have similar clustering properties to giant E's and S0's in that they are more centrally concentrated around the cluster centers than are spiral and irregular galaxies (Ferguson & Sandage 1989). In contrast, the bright nonnucleated dE's ($B_T < 17.5$) are distributed like the spirals and irregulars. (See also Binggeli, Tammann, & Sandage 1987; Ichikawa et al. 1988.)

The distribution of dE flattenings sets constraints on their three-dimensional shapes and therefore provides a clue to the origin of dwarf galaxies. Many studies have explored this point. Caldwell (1983) examined a small number of Virgo dE's and concluded that the flattening distribution was similar both to that of giant E's and to that of field irregular galaxies. This conclusion was also supported by Ichikawa et al. (1986) in their analysis of a significantly larger data set (69 dE's); though later, Ichikawa (1989) found no significant differences between the flattening distribution of dE's and E's and between that of nucleated and nonnucleated dE's. Ferguson & Sandage (1989) concluded that the flattening distributions of giant E's and nonnucleated dwarf E's were similar, but the flattenings of bright nonnucleated dE's were like those of the irregulars. Harris (1991) finds that the nonnucleated dE's are more elongated than the "generally round" nucleated systems.

Even with all this information handy, there are several reasons which motivated us to reexamine the flattenings of the Virgo dE's. First, nearly all the luminosities and axial ratios for the Virgo dE's in the VCC are based on photographic techniques, which can yield poor estimates of the total magnitude (Impey et al. 1988). Also, photographic surveys of giant E's for flattening estimates have usually overestimated the number of round galaxies (Fasano & Vio 1991; Ryden 1992; Ryden, Lauer, & Postman 1993) and can have significant systematic errors for galaxies as faint as dE's. Finally, the few studies of dwarf galaxies to use CCD imaging have not addressed the question of the distribution of flattenings, an important measure of intrinsic shapes since the dE's are typically too faint for kinematical studies.

For these reasons, we have embarked on a program to obtain high-quality images of Virgo dE's and irregulars to reexamine their properties and the connections (if any) between the different classes of galaxies. In this first paper, we report the results of an initial *R*-band CCD survey of 70 Virgo dE's. We first discuss the observations, data reduction, and surface photometry, then demonstrate that the Virgo dwarfs have a significantly flatter distribution than do giant ellipticals.

2. OBSERVATIONS AND DATA REDUCTION

We obtained images of 70 nucleated and nonnucleated Virgo dE's with the 1.8 m Perkins telescope[4] at Lowell Obser-

[1] National Science Foundation Young Investigator; ryden@payne.mps.ohio-state.edu.
[2] Visiting Observer, Lowell Observatory, Flagstaff, Arizona.
[3] Presidential Young Investigator; terndrup@payne.mps.ohio-state.edu.
[4] The Perkins Telescope is owned by Ohio Wesleyan University and is jointly operated by Lowell Observatory and The Ohio State University.

vatory on the nights of 1993 April 18–21 UT. We employed the Ohio State Imaging Fabry-Perot System (IFPS) configured in "direct" mode, without an etalon in the light path. The detector was the Lowell Observatory NCCD Tektronix chip (800 × 800 pixels), which in combination with the IFPS provides an unvignetted field of view of 5.'6 east–west and 6.'0 north–south at a scale of 0.''49 pixel^{-1}.

We selected our sample of dE's from the VCC by separately ordering the lists of the nucleated and nonnucleated dE's by total blue magnitude B_T; the lists specifically excluded those galaxies classified as "dE(?)" and included only those unambiguously identified by BST as Virgo cluster members. We observed approximately every third galaxy on both magnitude-sorted lists down to $B_T \sim 17.0$, which yielded a sample of 46 nucleated and 24 nonnucleated dE's. This method of selection was designed to reduce biases with respect to axial ratio.

The sampling statistics for our galaxies are summarized in Figure 1. The top panel shows (*unshaded histogram*) the number of dE's in the VCC down to $B_T = 17.5$ and (*shaded histogram*) the number of nucleated dE's. The central panel shows the number of nucleated dE's (*filled circles*) and nonnucleated dE's (*open circles*) that we observed. The lower panel displays the percentage of nucleated and nonnucleated dE's in our sample, where the symbols are as in the central panel. The overall sampling fraction is 33.5% of catalog dE's, more or less independent of B_T. The "bump" in the percentage of nonnucleated galaxies near $B_T = 15$ resulted from our observing nearly all of the very few bright nonnucleated dE's in the catalog.

All galaxies were observed through a (Cousins) R-band filter in a single exposure of 900 s, with the exception of VCC 128 and VCC 543, which were observed in two exposures of 600 s each. Only one night of the run was photometric, while the other nights had various amounts of thin cirrus. The seeing throughout the run, as measured from the FWHM of stellar images, averaged 2.''–2.''5.

All steps of the reduction and analysis were performed using the VISTA image processing package (Stover 1988). Raw images were first corrected for DC offset, which was measured by overscanning in rows and columns. The Lowell NCCD detector has a charge transfer efficiency slightly less than unity, which produces a bleeding of the charge level from the sky into the overscan regions. Consequently it was necessary to measure the DC offset using only the last 11 of the 32 pixels in the overscan regions. Inspection of several images did not reveal any structure in the overscan region other than the charge transfer problem, so we adopted a DC level for each frame equal to the mode of the pixels in the two 11 × 800 overscan areas. The images were then trimmed to remove vignetted portions.

The images were then divided by a flat field, composed of the median of eight high-signal twilight flats, each multiplicatively scaled to a common count level. The accuracy of the flat-field process was measured by examining two exposures of the Virgo Cluster field, equal in exposure time to those of the target galaxies (900 s), but which did not contain any of the galaxies. In both of these exposures, the level of the sky as determined by row or column cuts or by comparison of the modal value of various patches was constant to 0.1% rms.

Photometric calibration was available for the 17 galaxies observed on the one clear night of the run. The transformation to the Cousins system was obtained via 16 observations of

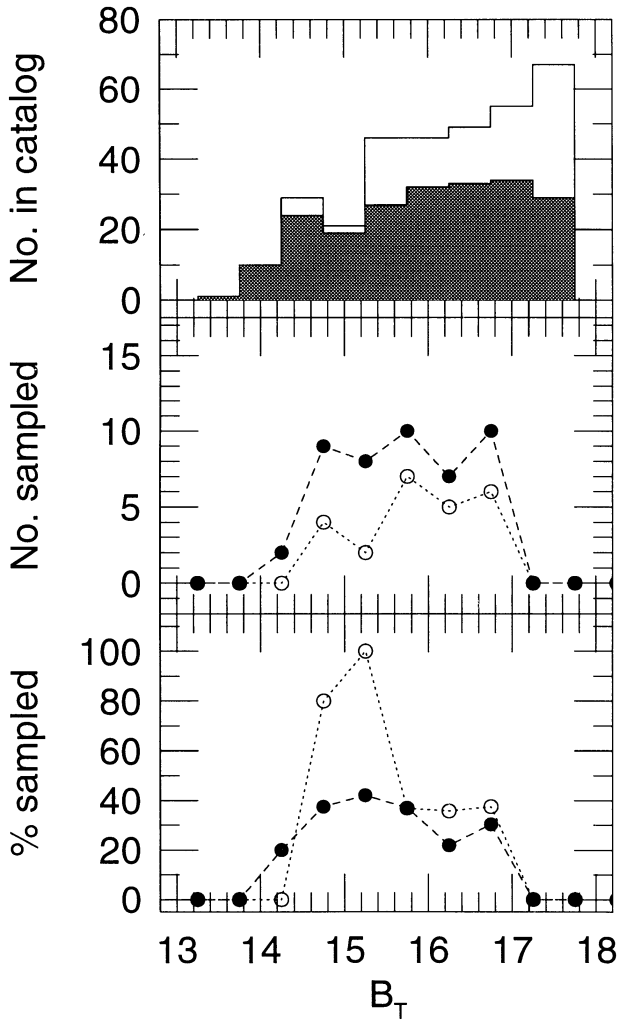

FIG. 1.—Sampling statistics for the galaxies we observed. The top panel shows (*unshaded histogram*) the number of dE's in the VCC down to $B_T = 17.5$ and (*shaded histogram*) the number of nucleated dE's. The central panel shows the number of nucleated dE's (*filled circles*) and nonnucleated dE's (*open circles*) that we observed. The lower panel displays the percentage of nucleated and nonnucleated dE's in our sample, where the symbols are as in the central panel.

eight standards in the list of Landolt (1983). A transformation of the form $R = r - 0.148X + \text{const}$ produced residuals of 0.018 mag rms; here X is the air mass and $r = -2.5 \log_{10}$ (counts s^{-1}) is the instrumental magnitude as measured within an aperture of diameter 11.''8. There was some evidence that the transparency varied systematically throughout the night at the 1% level, with the latter half of the night having the greater transparency. Because the residuals in the simplest transformation were so small, however, we decided not to apply a correction term involving UT. The mean sky level on the frames obtained during the photometric night was 20.78 ± 0.06 (σ) mag arcsec^{-1}. For comparison, a dark site such as Cerro Tololo has 21.23 mag arcsec^{-1} under ideal conditions (Geisler 1988).

3. DISTRIBUTION OF ELLIPTICITIES

We measured the surface brightness profiles of the target galaxies with the VISTA routine PROFILE (Lauer 1985). Each galaxy was modeled as a series of concentric ellipses,

yielding for each semimajor axis length a the surface brightness $\Sigma(a)$ and axial ratio $q \equiv b/a$, where b is the length of the semiminor axis. (We discuss deviations from elliptical isophotes below.) Before measurement, images of nearby stars were eliminated by replacing intensities higher than a local modal value with the mode. The sky level was determined on each frame by computing the mean value of the modal sky in four to six regions surrounding the target galaxy; typically the error in the sky level as judged by the rms scatter in the modal sky values was 0.3%.

Figure 2 displays the major-axis profiles (*left panels*) and position angles (*right panels*) of selected dE's that were observed on the one photometric night of the run. The surface brightness is expressed in R mag arcsec^{-1} and is displayed as a solid line with error bars. The error bars include photon statistics (dominant in the inner portions of the profile) and the uncertainty in the sky level. The position angles are in degrees from north through east and typically have errors for those galaxies with $\epsilon > 0.1$ of about 3° in the innner parts of the profile, increasing to 15° at the ends.

As has been noted several times before (Caldwell 1983; Binggeli et al. 1984; Ichikawa et al. 1986; Impey et al. 1988; Binggeli & Cameron 1991; James 1991), the profiles of most dE's are very nearly exponential over the full range over which they can be measured. We find, however, that a few galaxies classified as dE have profiles which are exponential at large radii but considerably brighter within 20″ of the core and therefore probably should have been classified as dS0 galaxies. In our sample the likely dS0's are VCC 543, 745, 1407, and 1491, representing about 6% of the sample.

For a direct comparison of the distribution of dE flattenings to those of giant E's (Ryden 1992) or brightest cluster galaxies (Ryden et al. 1993), we compute an intensity-weighted ellipticity $\bar{\epsilon}$ as follows. The luminosity between two adjacent isophotes with axial ratios $q \equiv b/a$ is

$$dL = 2\pi q a\left(1 + \frac{1}{2}\frac{d\ln q}{d\ln a}\right)\Sigma\, da\ . \tag{1}$$

The mean axis ratio $\bar{q}$ can then be defined as

$$\bar{q} = \frac{\int q\, dL}{\int dL}\ , \tag{2}$$

and the intensity-weighted ellipticity as $\bar{\epsilon} = 1 - \bar{q}$.

The integrals in equation (2) were computed from an inner cutoff radius a_i; inside of this radius the profile is dominated by seeing. We chose $a_i = 3''$ for all galaxies. Instead of computing equation (2) until the data ran out at large radii, we picked a fiducial radius a_0 to be the semimajor axis length at which the intensity profile $\Sigma(a_0) = 100$ counts. The value of $\bar{q}$ is nearly

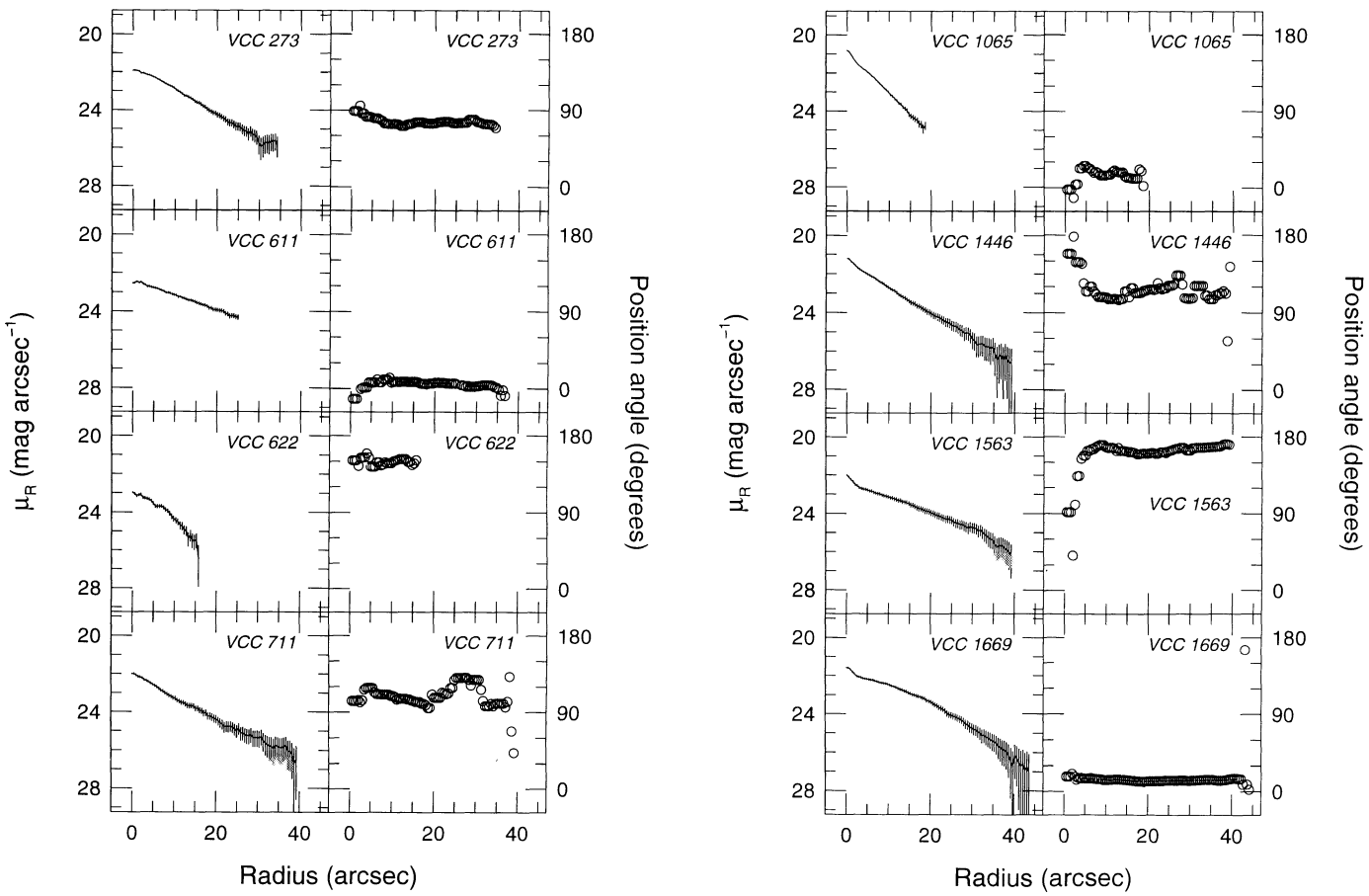

FIG. 2.—Representative major-axis profiles. Shown are (*left panels*) the surface brightness profiles in R mag arcsec^{-1} for selected galaxies from the one photometric night of our run, and (*right panels*) the run of position angle with radius. The error bars on the surface brightness include both photon statistics and errors in the sky level.

TABLE 1

ELLIPTICITIES OF VIRGO DWARFS

VCC	a_o(")	$\bar{\epsilon}$	$\epsilon(a_o)$	error	Note	VCC	a_o(")	$\bar{\epsilon}$	$\epsilon(a_o)$	error	Note	VCC	a_o(")	$\bar{\epsilon}$	$\epsilon(a_o)$	error	Note
128	27.2	0.15	0.24	0.06		1044	...	...	0.34	0.06	2	1649	28.8	0.23	0.28	0.04	
273	22.5	0.31	0.31	0.03	1	1065	17.0	0.10	0.16	0.04	1	1651	11.2	0.37	0.15	0.10	
319	...	...	0.04	0.04	1,2	1073	...	...	0.28	0.05	2	1669	29.4	0.55	0.58	0.03	1
421	15.1	0.16	0.22	0.04		1087	...	...	0.25	0.07	2	1677	12.5	0.24	0.16	0.05	
458	19.0	0.36	0.23	0.04		1104	31.8	0.28	0.33	0.04		1683	...	...	0.10	0.10	2
543	47.5	0.44	0.44	0.03		1122	49.6	0.53	0.64	0.03		1689	14.5	0.20	0.09	0.10	
545	23.7	0.22	0.20	0.03		1180	21.7	0.22	0.22	0.03		1698	25.3	0.47	0.35	0.05	
551	27.6	0.26	0.27	0.07		1223	18.5	0.42	0.41	0.06		1704	24.2	0.47	0.47	0.03	
592	19.6	0.39	0.33	0.06		1240	18.1	0.42	0.48	0.04		1743	30.9	0.51	0.40	0.05	
608	31.2	0.37	0.25	0.05		1264	...	...	0.22	0.06	2	1762	24.1	0.51	0.54	0.05	
611	...	...	0.47	0.07	1,2	1351	32.7	0.33	0.29	0.04		1767	23.0	0.30	0.36	0.05	1
622	11.8	0.45	0.49	0.03	1	1355	43.9	0.20	0.15	0.06		1803	24.3	0.07	0.19	0.11	
684	21.4	0.08	0.02	0.04	1	1407	33.7	0.15	0.15	0.03		1886	37.1	0.39	0.43	0.03	
711	21.6	0.14	0.04	0.03	1	1431	33.3	0.04	0.01	0.03		1919	5.6	0.20	0.14	0.06	
745	42.9	0.37	0.45	0.06		1432	15.8	0.12	0.18	0.03	1	1942	...	...	0.34	0.05	1,2
750	43.7	0.24	0.39	0.05		1446	25.2	0.09	0.08	0.03	1	1948	31.5	0.28	0.35	0.04	
753	23.1	0.10	0.11	0.04		1489	29.5	0.40	0.45	0.03		1991	33.6	0.25	0.21	0.03	
810	16.5	0.05	0.01	0.03	1	1491	34.6	0.22	0.33	0.07		2004	29.5	0.21	0.34	0.10	
816	...	...	0.41	0.06	2	1503	34.0	0.16	0.20	0.04	1	2008	...	...	0.54	0.03	2
817	...	...	0.10	0.06	2	1514	41.4	0.62	0.49	0.05		2042	26.0	0.11	0.12	0.03	
823	...	...	0.07	0.05	2	1539	27.0	0.11	0.05	0.04		2049	30.2	0.68	0.65	0.03	1
931	21.5	0.19	0.28	0.04		1563	28.4	0.30	0.35	0.02	1	2063	16.1	0.27	0.38	0.13	
933	17.3	0.33	0.37	0.05		1577	20.6	0.24	0.30	0.04		2090	33.2	0.51	0.44	0.05	
991	...	...	0.38	0.05	1,2												

NOTES.—(1) Observed under photometric conditions. (2) Galaxy image partly obliterated from bright stars, other galaxies or vignetting from guide probe. Ellipticity estimated as described in the text.

independent of the choice of a_0 since Σ typically falls off exponentially. The values of a_0 for each galaxy are displayed in Table 1. Because most of the galaxies were observed under nearly photometric conditions, the radius a_0 corresponds to a particular surface brightness, which for the galaxies observed in the best conditions is $R = 24.8$ mag arcsec^{-1}. Error estimates for $\bar{\epsilon}$ were derived by computing the variance in $\epsilon(a)$ with radius.

For 55 of the 70 galaxies we observed, it was possible to measure the radial profile down out to $\Sigma(a_0) = 100$ counts. The remaining galaxies could not be so measured because at large radii their images overlapped with those bright stars or adjacent galaxies, or were vignetted by the guide probe due to software errors in the algorithm for automatic guider placement. We estimated the ellipticities for these galaxies by measurement of b/a on contour plots of image intensity.

To demonstrate that the derived values of $\bar{\epsilon}$ are not sensitive to the value of a_0, we also list in Table 1 the ellipticity of the isophote with semimajor axis a_0, which we designate $\epsilon(a_0)$. The ellipticities measured off the contour plots are in the $\epsilon(a_0)$ column of Table 1. If galaxies were rounder in their bright inner regions, for example, we would find $\bar{\epsilon} < \epsilon(a_0)$. Figure 3 shows the correlation between $\bar{\epsilon}$ and $\epsilon(a_0)$. The solid line on the figure denotes identity. The mean difference $\bar{\epsilon} - \epsilon(a_0) = 0.00 \pm 0.08(\sigma)$; a scatter of 0.07 is expected from the listed errors. We therefore conclude that the dE's are, in general, not significantly rounder in their inner parts than they are at large radii.

The values of $\bar{\epsilon}$ that we derive are significantly different from those found from earlier photographic work. In Figure 4 we plot the correlation between $\bar{\epsilon}$ and the ellipticities in the VCC. (The catalog actually lists the logarithm of the major-to-minor axis ratio. We have converted their values into ellipticities.) Two features in this plot may be noted. The first is that the VCC contains a number of galaxies for which BST estimated $\epsilon = 0$, but which in fact have $0.03 \leq \bar{\epsilon} \leq 0.21$ with $\langle\bar{\epsilon}\rangle = 0.10$. This is reminiscent of the situation for giant E's (Ryden 1992), in which the number of round galaxies had been overestimated. Second, BST's estimates for ϵ are significantly larger than what we derive; for $\bar{\epsilon} > 0.1$, $\langle\bar{\epsilon} - \epsilon(\mathrm{BST})\rangle = 0.1$, which means that a galaxy classed, for example, as dE4 in the catalog is really more like dE3.

We have not been able to convince ourselves of the source of the systematic errors in the catalog ϵ. Figure 5 displays the difference (ours *minus* catalog) in ϵ as a function of the catalog total blue magnitude B_T. In this figure, nucleated E's are shown as open circles. The points with an $\times$ through them have $\epsilon(\mathrm{BST}) \equiv 0.0$, which all have positive differences in this plot because, as discussed above, their true ellipticities are

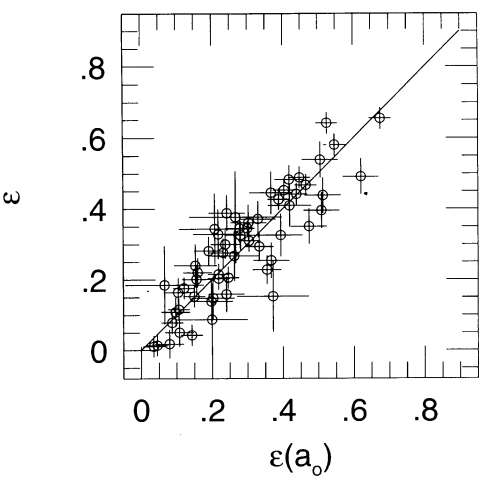

FIG. 3.—Comparison of the luminosity-weighted ellipticity $\bar{\epsilon}$ with the ellipticity of the isophote at the fiducial radius a_0, as defined in the text. The solid line denotes identity.

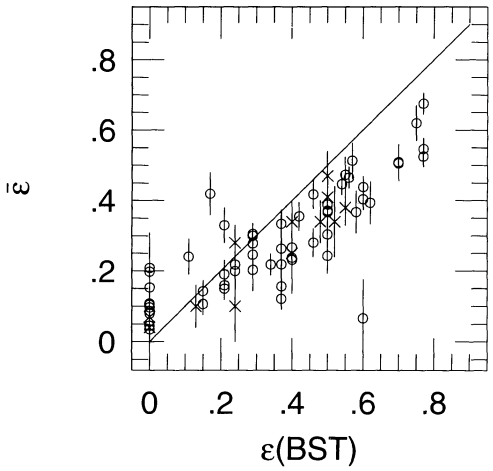

FIG. 4.—Comparison of our luminosity-weighted ellipticity (*open circles*) or estimates from contour plots (×'s) with axial ratios estimated by BST. The diagonal line is identity.

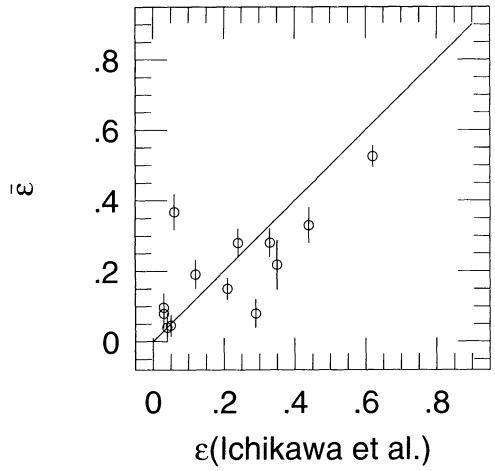

FIG. 6.—Comparison of our luminosity-weighted ellipticity to that tabulated by Ichikawa et al. (1986). The solid line denotes identity.

larger. Aside from these galaxies, there is no trend in $\bar{\epsilon} - \epsilon$(BST) with magnitude. BST had already noted that their measurements were flatter, on average, than those of de Vaucouleurs & Pence (1979).

In Figure 6 we compare our values of $\bar{\epsilon}$ with those tabulated by Ichikawa et al. (1986). There is considerable scatter between the two determinations, but no significant differences between our values and their photographically derived ellipticities.

Figure 7 displays (*heavy solid line*) the cumulative distribution function $F(\epsilon)$ for the 57 dE's in Virgo with measured $\bar{\epsilon}$. Also shown (*light solid line*) are the distribution function of 165 giant E's (Ryden 1992) and (*dotted line*) that of brightest cluster E's (Ryden et al. 1993). The dE distribution is clearly flatter than the other two: as measured by a Kolmogorov-Smirnoff test, the probabilities that the dE sample is drawn from the giant E or brightest cluster E samples are only $P_{KS} = 2.8 \times 10^{-3}$ and $P_{KS} = 1.2 \times 10^{-4}$. The Mann-Whitney (M-W) statistic (Seigel 1956), which compares the medians of two distributions, is $P_{MW} = 1.6 \times 10^{-4}$ for these samples, also indicating that the dE's have a distinct flattening distribution from that of brighter galaxies. Note that our derived distribution of ellipticities is *flatter* than that of giant E's even though we measure the dE's to be *rounder* than in the catalog.

We also compared the dE flattenings to the distribution of flattening in E's from Franx, Illingworth, & de Zeeuw (1991), who compiled flattenings from a large sample of CCD observations from the literature and from their own observations. Their distribution is *slightly* flatter than in Ryden (1992), mainly because there are a few more galaxies of extreme flattening in their compilation. The differences in flattening between the two samples of E's become statistically significant only for $\epsilon > 0.6$. From Figure 7 it is apparent that the dE distribution is markedly flatter than that for E's at rounder axial ratios than this. We therefore believe that our conclusion that the dE's are flatter than E's is not dependent on the choice of elliptical sample.

Given that there have been several earlier claims (cited above) that the distribution of dE ellipticities matches that of

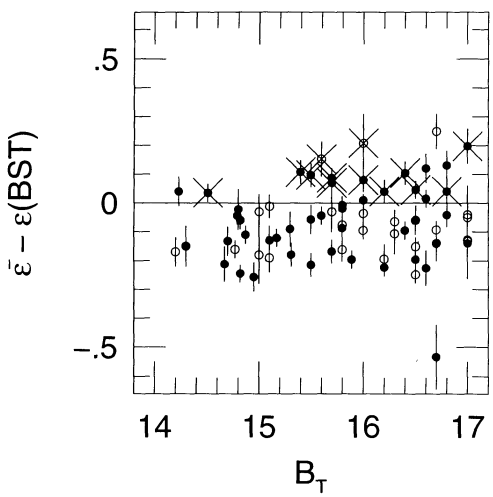

FIG. 5.—Difference between our intensity-weighted ellipticity and the value tabulated in the VCC as a function of total blue magnitude B_T. Open and filled points designate nonnucleated and nucleated dE's, respectively. Points with an × through them are round galaxies ($\epsilon \equiv 0.0$) in the VCC.

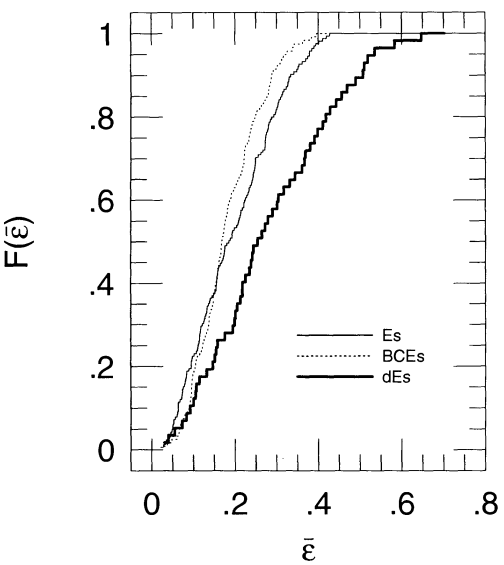

FIG. 7.—Cumulative distribution function for our sample of dE's (*heavy solid line*) compared to that for giant E's and brightest cluster ellipticals.

giant E's, our demonstration that they are distinct indicates that the formation mechanism for the two classes of galaxies was not identical. We explore the implications for the formation of the dE's below. In the meantime, we now proceed to justify our conclusion by examining the data set in various ways.

Figure 8 compares the distribution for the 57 galaxies with measured $\bar{\epsilon}$ to that for all 70 galaxies in the sample; for the other 15 we used the estimated ellipticity from contour plots. The distribution functions are virtually identical. We can therefore continue our analysis combining-weighted and estimated ellipticities of the full data set.

First, we need to justify that we performed an unbiased sample of the VCC catalog. It could be, after all, that we inadvertently picked out galaxies in a nonuniform fashion so that the largest possible range of ϵ was included in the sample, which would produce a flatter distribution function (we actually did sample the galaxies for a large range of ϵ on the first night of the run, but fortunately had enough time to go back and, as outlined above, obtain an unbiased sample).

Figure 9 compares $F(\epsilon)$ for the 70 galaxies of our sample to that of the 131 dE's with $B_T < 17.0$ in the VCC that we did not observe. In this figure, the values ϵ are those tabulated in the VCC, *not* the ones we derived. This produces a large step in the distribution function at $\epsilon = 0.0$, caused by the catalog listing most galaxies with $\epsilon < 0.15$ as $\epsilon = 0.0$. The K-S probability for these two distributions is $P_{KS} = 0.65$, while the M-W statistic is 0.110. We therefore conclude that our sample of the VCC is unbiased over ellipticity. It is also straightforward to demonstrate (not shown) that the sample of both nucleated and nonnucleated dE's are equally free of bias over ellipticity.

There have been several suggestions in the literature (e.g., Norman 1985) that nucleated dE's should be rounder than their nonnucleated counterparts. Impey et al. (1988) found no such difference with small samples. We test this by plotting (Fig. 10) the distribution functions for the nucleated and nonnucleated dE's separately, along with the distribution function for giant E's. The nucleated dE's are indeed rounder than the nonnucleated galaxies—the statistics for this comparison are

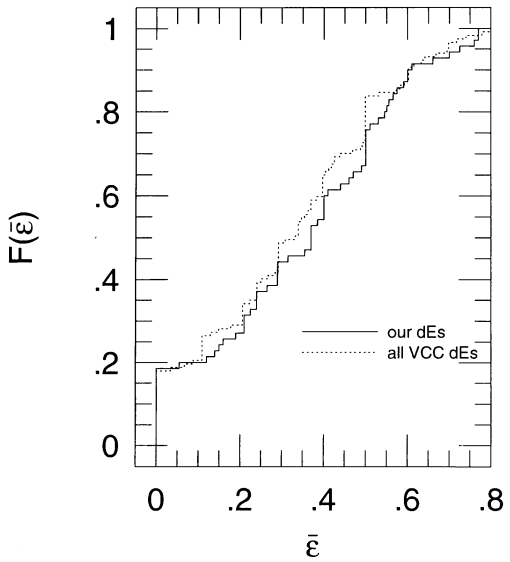

FIG. 9.—Distribution for sampled and unsampled dE's in VCC units

$P_{KS} = 0.132$ and $P_{MW} = 0.030$—but *both* distributions are flatter than that of giant E's.

The distribution of $\bar{\epsilon}$ provides constraints on the distribution of three-dimensional shapes of the dE's. Following Ryden (1992), we assume that the dE's are triaxial ellipsoids with axis ratios $1:\beta:\gamma$, and that the distribution of intrinsic axis ratios $f(\beta, \gamma)$ has an isotropic Gaussian form, with a peak at the position β_0, γ_0 and width σ_0. Specifically, we assume

$$f(\beta, \gamma) \propto \exp\left[-\frac{(\beta - \beta_0)^2 - (\gamma - \gamma_0)^2}{2\sigma_0^2}\right], \qquad (3)$$

with the constraint $0 \leq \gamma \leq \beta \leq 1$. Then for a range of β_0, γ_0, σ_0 we can calculate the distribution of projected ellipticities and compare this to the observed distribution through a K-S test.

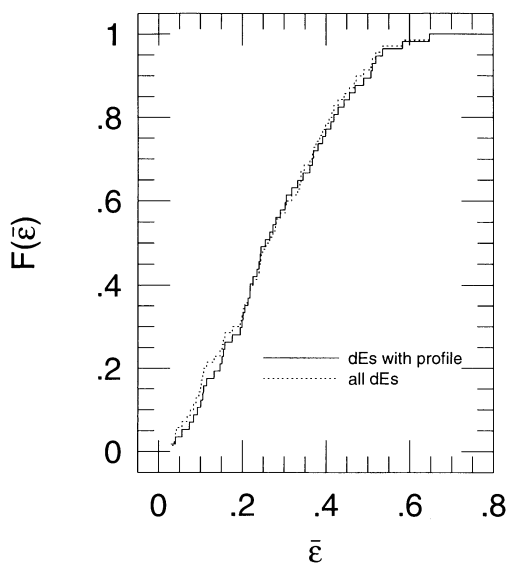

FIG. 8.—Distribution function for the all sampled dE's (*solid line*) compared to the distribution of dE's with accurately measured profiles (*dotted line*).

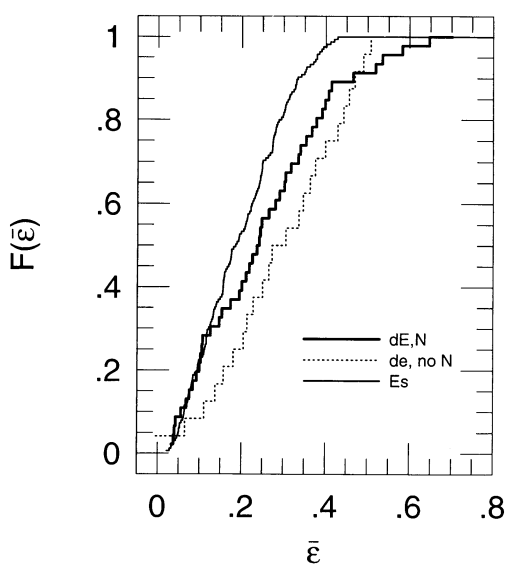

FIG. 10.—Flattening distribution of nucleated and nonnucleated dwarfs considered separately with normal E's.

First we considered both nucleated and nonnucleated dE's together. The best fitting distribution has $\beta_0 = 0.95$, $\gamma_0 = 0.54$, and $\sigma_0 = 0.16$. The reduced χ^2 for this fit is $\chi^2/\nu = 0.35$. Isoprobability contours around the peak of the model distribution are shown in Figure 11.

We have also derived estimates for the intrinsic shapes of the nucleated and nonnucleated dE's separately, though the results of the calculation are more uncertain because of the smaller sample sizes. The best-fitting model for the nucleated dwarfs has a broad range of intrinsic shapes, with $\beta_0 = 0.96$, $\gamma_0 = 0.88$, and $\sigma_0 = 0.32$ with $\chi^2/\nu = 0.70$. For the nonnucleated dwarfs, we derive $\beta_0 = 0.81$, $\gamma_0 = 0.45$, and $\sigma_0 = 0.00$ with $\chi^2/\nu = 0.23$. The equivalent solution for 171 giant E's is (Ryden 1992) $\beta_0 = 0.98$, $\gamma_0 = 0.69$, and $\sigma_0 = 0.11$. At face value, these statistics imply that the nonnucleated dEs can all have the same intrinsic shape, which is significantly flatter and somewhat more triaxial than the nucleated dwarfs. We hestitate to call this a firm conclusion, since a model which fits the entire sample ($\beta_0 = 0.95$, $\gamma_0 = 0.54$, $\sigma_0 = 0.16$) yields a reduced χ^2 of 1.83 and 1.63 when applied to the nucleated and nonnucleated dE's, and so cannot be rejected at the 90% confidence level. The moral of the story is that more data are needed to distinguish the distributions of intrinsic shapes of the nucleated and nonnucleated Virgo dE's.

Finally, we make two other observations about the dE's. First, we note that most of the dE's do not have significant isophotal twists in their profiles, which are very common in normal E's. For each profile, we computed a weighted deviation from the value of $\bar{\epsilon}$, where the weights are the inverse of the error in the position angle. We find that no more than 25% of the dE's have isophotal twists in excess of 10°; in comparison, Rampazzo & Buson (1990) find that 70% of giant E's have isophotal twists of this size.

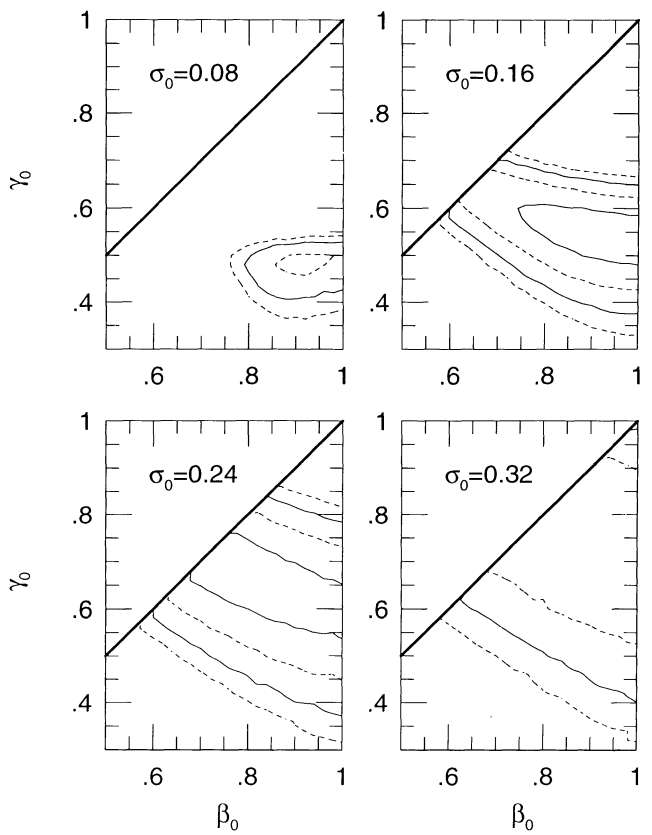

FIG. 11.—Isoprobability contours, as measured by a K-S test on four slices through the (β_0, γ_0, σ_0) parameter space. The fit is to our entire sample of 70 nucleated and nonnucleated dE's. Contours are drawn at the probability levels $P_{KS} = 0.01$, 0.1, and 0.5.

Second, we note that few, if any, of the brightest dE's in our sample show significant "boxy" or "disky" deviations from elliptical isophotes. For a subsample of 10 bright dE's, not including the possible dS0 galaxies discussed above, we computed the radial profiles including terms expressing fractional luminosity deviations from perfect ellipses. The deviation of an isophote from an ellipse can be quantified by doing a Fourier expansion around the best-fitting isophote, in the form (Carter 1978)

$$I(\theta) = I_0 + \sum_{n \geq 3} (A_n \cos n\theta + B_n \sin n\theta) , \quad (4)$$

where θ is the position angle measured from the major axis of the ellipse. The luminosity deviations A_n and B_n at a semimajor axis a can be converted to fractional radial deviations a_n/a and b_n/b through the relations

$$\begin{aligned} a_n/a &= -A_n[a(dI_0/da)] , \\ b_n/b &= -B_n[a(dI_0/da)] . \end{aligned} \quad (5)$$

This was the approach used by Lauer (1985), Jedrzejewsky (1987a), Franx, Illingworth, & Heckman (1989), and Peletier et al. (1990). As summarized in reviews by Jedrzejewsky (1987b), Nieto (1988), Kormendy & Djorgovski (1989), and Bender (1990), about one-third show boxiness at the level of $a_4/a < -0.5\%$, while another third show diskiness at the $a_4/a > 0.5\%$, while only one-third show no significant deviations from perfect elliptical isophotes. In the 10 Virgo dE's we examined in detail, none showed $|a_4/a| > 0.5\%$, which suggests that isophotal twisting is a rarer phenomenon than it is among E's.

4. DISCUSSION

Dwarf elliptical galaxies (dE's) and "normal" elliptical galaxies (E's) are very different in their properties. For instance, dE's have a low central surface brightness and nearly exponential luminosity profiles. E's have high surface brightness and luminosity profiles which are well described by an $r^{1/4}$ profile. As we have shown in this paper, dE's are flatter, on average, than E's. One property that dE's and E's have in common is the elliptical shape of their isophotes. But even here, it appears that dE's are more flattened ellipticals than E's. Furthermore, none of the dwarfs studied in this paper showed strong disky or boxy distortions of their isophotes, but in a typical sample of bright elliptical galaxies, approximately one-third show measurable boxiness of their isophotes and approximately one-third show measurable diskiness (Bender, Döbereiner, & Möllenhoff 1988). This suggests that the dE's have few or no embedded disks.

The differences between dE's and E's are the result of differences in their formation and evolution. Giant elliptical galaxies, with their high surface brightness, can form by the merger of smaller galaxies. Dwarf elliptical galaxies, however, have a much lower density and specific binding energy (Saito 1979a); they must rely on a different mechanism for their creation. One proposed scenario for the creation of dE's is through the removal of gas from a gas-rich progenitor. The gas could be removed by ram-pressure stripping (Einasto et al. 1974; Gerola, Carnevali, & Salpeter 1983; Lin & Faber 1983)

or by a supernova-driven galactic wind, after a burst of star formation (Larson 1974; Saito 1979b; Dekel & Silk 1986; Vader 1986, 1987; Yoshii & Arimoto 1987; Angeletti & Giannone 1990).

If dE's are formed by gas stripping, then what did their progenitors look like? One suggestion has been that the progenitors were dwarf irregulars (Einasto et al. 1974; Lin & Faber 1983). Some photographic studies (Caldwell 1983; Ferguson & Sandage 1989) have compared the flattening distribution of dE's and that of irregular galaxies, and have shown that they are similar. As we mentioned earlier in this paper, however, photographic estimates of the ellipticity of galaxies are not always of sufficient accuracy to determine the distribution of shapes. We plan to explore the connections, if any, between dE's and the dwarf irregulars in future observing runs.

Of course, it is possible that some or all dE's form by some other means. For instance, dwarf galaxies with low surface brightness can form out of clumps of tidal debris, ejected from the close encounter of two bright galaxies (Gerola et al 1983; Barnes & Hernquist 1992). Whether dE's were formed in tidal encounters, or through the stripping of gas from a progenitor, or through some other, yet unguessed mechanism, the formation and subsequent modification of dE's must lead to the observed, relatively flat shapes of dE's.

We wish to thank Ray Bertram for his able assistance at the telescope and Mark Wagner for his hospitality during our run at Lowell Observatory. D. T. acknowledges helpful suggestions and comments by Nelson Caldwell, Ruth Peterson, and Richard Pogge.

REFERENCES

Angeletti, L., & Giannone, P. 1990, A&A, 234, 53
Barnes, J. E., & Hernquist, L. 1992, Nature, 360, 715
Bender, R. 1990, in Dynamics and Interactions of Galaxies, ed. R. Wielen (Berlin: Springer-Verlag), 232
Bender, R., Döbereiner, S., & Möllenhoff, C. 1988, A&AS, 74, 385
Binggeli, B., & Cameron, L. M. 1991, A&A, 252, 27
Binggeli, B., Sandage, A., & Tammann, G. A. 1985, AJ, 90, 1681 (BST)
Binggeli, B., Sandage, A., & Tarenghi, M. 1984, AJ, 89, 64
Binggeli, B., Tammann, G. A., & Sandage, A. 1987, AJ, 94, 251
Caldwell, N. 1983, AJ, 88, 804
Carter, D. 1978, MNRAS, 212, 767
Dekel, A., & Silk, J. 1986, ApJ, 303, 39
de Vaucouleurs, G., & Pence, W. D. 1979, ApJS, 40, 425
Einasto, J., Saar, E., Kaasik, A., & Chernin, A. D. 1974, Nature, 252, 111
Fasano, G., & Vio, R. 1991, MNRAS, 249, 629
Ferguson, H. C., & Sandage, A. 1989, ApJ, 346, L53
Franx, M., Illingworth, G., & de Zeeuw, T. 1991, ApJ, 383, 112
Franx, M., Illingworth, G., & Heckman, T. 1989, AJ, 98, 538
Geisler, D. 1988, NOAO Newsletter, 13, 22
Gerola, H., Carnevali, P., & Salpeter, E. E. 1983, ApJ, 268, L75
Harris, W. E. 1991, PASP, 103, 32
Ichikawa, S.-I. 1989, AJ, 97, 1600
Ichikawa, S.-I., Okamura, S., Kodaira, K., & Wakamatsu, K.-I. 1988, AJ, 96, 62
Ichikawa, S.-I., Wakamatsu, K.-I., & Okamura, S. 1986, ApJS, 60, 475
Impey, C., Bothun, G., & Malin, D. 1988, ApJ, 330, 634
James, P. 1991, MNRAS, 250, 544
Jedrzejewski, R. I. 1987a, MNRAS, 226, 747
———. 1987b, in IAU Symp. 127, Structure and Dynamics of Elliptical Galaxies, ed. T. de Zeeuw (Dordrecht: Reidel), 257
Kormendy, J., & Djorgovski, S. 1989, ARA&A, 27, 235
Landolt, A. U. 1983, AJ, 88, 439
Larson, R. B. 1974, MNRAS, 169, 229
Lauer, T. R. 1985, ApJS, 57, 473
Lin, D. N. C., & Faber, S. M. 1984, ApJ, 266, L21
Nieto, J.-L. 1988, in Segunda Reunion Regional Sobre Astronomia Extragalactica, ed. J. Sersic et al. (Cordoba: Academia Nacional de Ciencias), 239
Norman, C. A. 1985, in Star Forming Dwarf Galaxies and Related Objects, ed. D. Knuth, T. X. Thuan, & J. T. T. Van (Gif sur Yvette, France: Ed. Frontiéres), 477
Peletier, R. F., Davies, R. L., Illingworth, G. D., Davis, L. E., & Cawson, M. 1990, AJ, 100, 1091
Rampazzo, R., & Buson, L. M. 1990, A&A, 236, 25
Reaves, G. 1956, AJ, 61, 69
———. 1983, ApJS, 53, 375
Ryden, B. S. 1992, ApJ, 396, 445
Ryden, B. S., Lauer, T. R., & Postman, M. 1993, ApJ, 410, 515
Saito, M. 1979a, PASJ, 31, 181
———. 1979b, PASJ, 31, 193
Seigel, S. 1956, Nonparametric Statistics for the Behavioral Sciences (New York: McGraw Hill)
Stover, R. J. 1988, in Instrumentation for Ground-Based Optical Astronomy, ed. L. B. Robinson (New York: Springer-Verlag), 443
Vader, J. P. 1986, ApJ, 305, 669
———. 1987, ApJ, 317, 128
van den Bergh, S. 1986, AJ, 91, 271
Yoshii, Y., & Arimoto, N. 1987, A&A, 188, 13